Quantitative biokinetics of titanium dioxide nanoparticles after intravenous injection in rats (Part 1)

Journal:	*Nanotoxicology*
Manuscript ID	TNAN-2016-0176.R2
Manuscript Type:	Original Article
Date Submitted by the Author:	n/a
Complete List of Authors:	Kreyling, Wolfgang; Helmholtz Center Munich – German Research Center for Environmental Health, Comprehensive Pneumology Center, Institute of Lung Biology and Disease; Helmholtz Center Munich – German Research Center for Environmental Health , Institute of Epidemiology 2 Holzwarth, Uwe; Joint Research Centre, Institute for Health and Consumer Protection Haberl, Nadine; Helmholtz Center Munich – German Research Center for Environmental Health , Comprehensive Pneumology Center, Institute of Lung Biology and Disease Kozempel, Ján; Joint Research Centre, Institute for Health and Consumer Protection Hirn, Stephanie; Helmholtz Center Munich – German Research Center for Environmental Health , Comprehensive Pneumology Center, Institute of Lung Biology and Disease, Wenk, Alexander; Helmholtz Center Munich – German Research Center for Environmental Health , Comprehensive Pneumology Center, Institute of Lung Biology and Disease Schleh, Carsten; Helmholtz Center Munich – German Research Center for Environmental Health, Comprehensive Pneumology Center, Institute of Lung Biology and Disease Schäffler, Martin; Helmholtz Center Munich – German Research Center for Environmental Health, Comprehensive Pneumology Center, Institute of Lung Biology and Disease Lipka, Jens; Helmholtz Center Munich – German Research Center for Environmental Health , Comprehensive Pneumology Center, Institute of Lung Biology and Disease

	Semmler-Behnke, Manuela; Helmholtz Center Munich – German Research Center for Environmental Health , Comprehensive Pneumology Center, Institute of Lung Biology and Disease Gibson, Neil; Joint Research Centre, Institute for Health and Consumer Protection
Keywords:	Size-selected, radiolabeled titanium dioxide nanoparticles, intravenous injection, accumulation in organs and tissues, translocation across organ membranes, Hepato biliary nanoparticle clearance
Abstract:	Submicrometer TiO2 particles, including nanoparticulate fractions, are used in an increasing variety of consumer products, as food additives and drug delivery applications are envisaged. Beyond exposure of occupational groups this entails an exposure risk to the public. However, nanoparticle translocation from the organ of intake and potential accumulation in secondary organs is poorly understood and in many investigations excessive doses are applied. The present study investigates the biokinetics and clearance of a low single dose (typically 40-400 µg/kg BW) of 48V-radiolabeled, pure TiO2 anatase nanoparticles ([48V]TiO2NP) with a median aggregate/agglomerate size of 70 nm in aqueous suspension after intravenous injection into female Wistar rats. Biokinetics and clearance were followed from 1-hour to 4-weeks. The use of radiolabeled nanoparticles allowed a quantitative [48V]TiO2NP balancing of all organs, tissues, carcass and excretions of each rat without having to account for chemical background levels possibly caused by dietary or environmental titanium exposure. Highest [48V]TiO2NP accumulations were found in liver (95.5%ID on day-1), followed by spleen (2.5%), carcass (1%), skeleton (0.7%) and blood (0.4%). Detectable nanoparticle levels were found in all other organs. The [48V]TiO2NP content in blood decreased rapidly after 24h while the distribution in other organs and tissues remained rather constant until day-28. The present biokinetics study is part 1 of a series of studies comparing biokinetics after three classical routes of intake (intravenous (IV) injection (part 1), ingestion (part 2), intratracheal instillation (part 3)) under identical laboratory conditions, in order to verify the common hypothesis that IV-injection is a suitable predictor for the biokinetics fate of nanoparticles administered by different routes. This hypothesis is disproved by this series of studies.

Quantitative biokinetics of titanium dioxide nanoparticles after intravenous injection in rats (Part 1)

Wolfgang G. Kreyling*[#§], Uwe Holzwarth[+], Nadine Haberl*, Ján Kozempel[+1], Stephanie Hirn*, Alexander Wenk*[2], Carsten Schleh*[3], Martin Schäffler*, Jens Lipka*, Manuela Semmler-Behnke*[4] and Neil Gibson[+]

* Helmholtz Center Munich – German Research Center for Environmental Health Comprehensive Pneumology Center, Institute of Lung Biology and Disease, Ingolstaedter Landstrasse 1,D-85764 Neuherberg / Munich, Germany

[#] Helmholtz Center Munich – German Research Center for Environmental Health, Institute of Epidemiology 2, Ingolstaedter Landstrasse 1, D-85764 Neuherberg / Munich, Germany

[+] European Commission, Joint Research Centre, Directorate F – Health, Consumers and Reference Materials, Via E. Fermi 2749, I-21027 Ispra (VA), Italy

[§] Corresponding author:

Wolfgang G. Kreyling
Institute of Epidemiology 2
Helmholtz Center Munich - German Research Center for Environmental Health
Ingolstaedter Landstrasse 1
D-85764 Neuherberg / Munich
Germany
phone: +49 89 2351 4817;
E-mail address: Kreyling@helmholtz-muenchen.de

[1] Current address: Czech Technical University in Prague, Faculty of Nuclear Sciences and Physical Engineering, Břehová 7, CZ-11519 Prague 1, Czech Republic
[2] Current address: Dept. Infrastructure, Safety, Occupational Protection, German Research Center for Environmental Health, D-85764 Neuherberg / Munich, Germany
[3] Current address: Abteilung Gesundheitsschutz, Berufsgenossenschaft Holz und Metall, D-81241 München, Germany
[4] Current address: Bavarian Health and Food Safety Authority, D-85764 Oberschleissheim, Germany

Keywords

Size-selected, radiolabeled titanium dioxide nanoparticles; intravenous injection, accumulation in organs and tissues, translocation across organ membranes, Hepato biliary nanoparticle clearance

Abstract

Submicrometer TiO_2 particles, including nanoparticulate fractions, are used in an increasing variety of consumer products, as food additives and drug delivery applications are envisaged. Beyond exposure of occupational groups this entails an exposure risk to the public. However, nanoparticle translocation from the organ of intake and potential accumulation in secondary organs is poorly understood and in many investigations excessive doses are applied.

The present study investigates the biokinetics and clearance of a low single dose (typically 40-400 µg/kg BW) of ^{48}V-radiolabeled, pure TiO_2 anatase nanoparticles ([^{48}V]TiO_2NP) with a median aggregate/agglomerate size of 70 nm in aqueous suspension after intravenous injection into female Wistar rats. Biokinetics and clearance were followed from 1-hour to 4-weeks. The use of radiolabeled nanoparticles allowed a quantitative [^{48}V]TiO_2NP balancing of all organs, tissues, carcass and excretions of each rat without having to account for chemical background levels possibly caused by dietary or environmental titanium exposure.

Highest [^{48}V]TiO_2NP accumulations were found in liver (95.5%ID on day-1), followed by spleen (2.5%), carcass (1%), skeleton (0.7%) and blood (0.4%). Detectable nanoparticle levels were found in all other organs. The [^{48}V]TiO_2NP content in blood decreased rapidly after 24h while the distribution in other organs and tissues remained rather constant until day-28.

The present biokinetics study is part 1 of a series of studies comparing biokinetics after three classical routes of intake (intravenous (IV) injection (part 1), ingestion (part 2), intratracheal instillation (part 3)) under identical laboratory conditions, in order to verify the common hypothesis that IV-injection is a suitable predictor for the biokinetics fate of nanoparticles administered by different routes. This hypothesis is disproved by this series of studies.

Introduction

Submicron titanium dioxide particles are increasingly used in food additives, in cosmetics and personal care products such as tooth paste, as UV-absorbers in sunscreen (Jia, 2008), and in other products such as pigments or fillers in paints, inks, and ceramics (Christensen, 2011). Their antimicrobial and even antiviral effects make them advantageous in water and air disinfection (Li, 2008). An analysis of (Weir, 2012) showed that approximately one third of the number of TiO_2 particles in common food products are nano-sized (<100 nm). (Peters, 2014) recently confirmed in 27 food items and personal care products that between 10% and 25% of the TiO_2 particles exhibit dimensions below 100 nm. Despite the extraordinary growth of use and applications of titanium dioxide nanoparticles (TiO_2NP) it is still unclear whether this entails health risks, especially for subjects occupationally exposed to inhalation of TiO_2NP during manufacturing and handling (Christensen, 2011) and when considering their high biopersistence and long-term retention known for 2-3 decades as reviewed by Shi and co-workers (Shi, 2013).

Recently medical applications of TiO_2NP for drug delivery have also been envisaged (Carlander, 2016), e.g., for restenosis treatment (Gu, 2013), making use of their physical properties for light-controlled drug release (Wang, 2015) or ultrasound cancer treatment (Ninomiya, 2014). On the other hand the release and fate of nanosized fractions of wear corrosion debris from orthopedic and dental titanium implants has become a concern (Matusiewicz, 2014).

Numerous *in vivo* and *in vitro* studies describe adverse effects in the mammalian organism but the results are not yet conclusive. One important issue is the dose of intravenously administered TiO_2NP when studying the behaviour of nanoparticles that reach systemic circulation. Doses of 10 mg/kg body weight (BW) and more have been reported. However, the question arises as to whether the results achieved with such high doses are still representative for the biodistribution that can be expected for much smaller quantities that

may reach systemic circulation following realistic exposure scenarios. Given our concern about excessive doses we refer to several studies which report biodistribution data (Fabian, 2008) (Patri, 2009) (Xie, 2011) (Geraets, 2014) and a likelihood of pro-inflammatory (Fabian, 2008) (Setyawati, 2013), genotoxic (Louro, 2014), immunotoxic (Auttachoat, 2013) as well as fetotoxic (Yamashita, 2011) responses to IV-injected TiO_2NP at high doses, with and without measurements during a recovery time.

Interestingly, an electron-microscopic study on the micro-biokinetics of 40 nm gold nanoparticles in the liver of mice after administration of 1.4 mg/kg BW (Sadauskas, 2009) found most of the nanoparticles in lysosomal / endosomal vacuoles of Kupffer cells, but the number of Kupffer cells containing nanoparticles decreased over time, while the nanoparticle load in the vacuoles increased since the overall nanoparticle clearance out of the liver was very low (Sadauskas, 2009). In our low-dose IV-injection study of monodisperse 18 nm gold nanoparticles (30 µg/kg BW) we confirmed the nanoparticle presence in Kupffer cells together with additional nanoparticles in sinusoidal endothelial cells and hepatocytes (Hirn, 2011). A recent comprehensive review addressed these issues in more detail (Shi, 2013). Furthermore, biokinetics data obtained from IV-injected engineered TiO_2NP are controversial since some reports note accumulation in organs after IV-injection, whereas others only note liver retention, depending very much on the sensitivity of the detection methodology used (Shi, 2013).

In the present series of three biokinetics studies we performed quantitative biokinetics studies in female rats by applying radiolabeled, engineered, commercially available TiO_2 anatase agglomerated/aggregated nanoparticles. After size selection of a true nano-fraction with a hydrodynamic diameter of about 70nm single doses of aqueous [^{48}V]TiO_2NP suspensions were applied by three routes of intake: intratracheal instillation (Kreyling, submitted-a) , intra-oesophageal instillation (gavage) (Kreyling, submitted-b), and in the present first part by intravenous injection. By using nanoparticles radiolabeled with the gamma-emitting

radionuclide ^{48}V, a high sensitivity is achieved over five orders of magnitude which is not affected by chemical background levels that might be caused by dietary and environmental titanium exposure of the animals. Moreover, no chemical processing of the biological specimens is required for subsequent γ-spectrometry and a complete [^{48}V]TiO_2NP balancing of all organs, tissues, carcass and excretions can be performed even for low administered doses. However, using the ^{48}V radiolabel, which is chemically different from the element Ti, requires stable integration into the NP matrix and careful control of labeling stability *in vivo*. Therefore, we conducted additional auxiliary biokinetics studies to quantify any release of the label for each organ and corrected the biokinetics data accordingly.

For each of these routes of intake quantitative biokinetics studies were performed by serial biodistribution analyses at five different retention time points between one hour and 28 days after application in order to determine the accumulated and retained nanoparticle doses in different organs of interest, selected tissues and body fluids, and also to provide a complete overview of the fate of the applied [^{48}V]TiO_2NP in the entire organism by additional evaluations of the carcass and the entire fecal and urinary excretion of each animal. The entire nanoparticle distribution is balanced in each animal and not normalized to a nominally administered nanoparticle dose loaded in a syringe, which (as reported below) may differ appreciably from the dose effectively delivered to an animal. Only such a quantitative approach can provide a detailed overview of the nanoparticle biokinetics and fate, whereas biokinetics studies focusing on a few organs of interest cannot provide sufficient information for a comprehensive understanding of the nanoparticle transport and accumulation processes within the organism.

The IV-injection study was carried out firstly to check the hypothesis that IV-injection may be a suitable surrogate approach for the biokinetics after oral or respiratory delivery of nanoparticles, and secondly to provide a quantitative biokinetics assay for a better understanding of targeted delivery of TiO_2NP-based drugs via the circulation. Since we knew

from previous biokinetics studies on a suite of monodisperse gold nanoparticles (AuNP) administered via the same three routes (Kreyling, 2011, Hirn, 2011, Kreyling, 2014, Schleh, 2012) and after inhalation of 20 nm iridium nanoparticles (IrNP) (Kreyling, 2002, Semmler, 2004, Semmler-Behnke, 2007) or 20 nm elemental carbon nanoparticles (ECNP) (Kreyling et al., 2011), that the accumulation dynamics occurs rather rapidly during the first 24-hours we chose three time points of investigations – 1h, 4h, 24h – in order to study the rapid accumulation dynamics observed previously, followed by two time points at 7d and 28d in order to assess possible slower processes of accumulation, redistribution and clearance.

Materials and Methods

Radiolabeling and size selection of TiO_2NP

Two batches of 20 mg ST-01 TiO_2NP were irradiated with a protons at a beam current of 5 μA. One, with an activity concentration of 1.0 MBq/mg (^{48}V-activity per TiO_2 mass), was used for the 1h, 4h and 24h retention experiments. The second one was irradiated on five consecutive days, yielded an activity concentration of 2.35 MBq/mg and was used for the 7d and 28d retention experiments. At these radioactivity concentrations the atomic ratio of ^{48}V:Ti in the nanoparticles is about 2.6×10^{-7} and 6.2×10^{-7}, respectively. Since proton bombardment and the chemical difference of the radiolabel, may result in a non-perfect integration of the ^{48}V in the TiO_2 matrix the [^{48}V]TiO_2NP were repeatedly washed to remove released ^{48}V-ions.

Size selection was performed in a repeated sequence of nanoparticle suspension, ultrasound homogenization, washing by centrifugation and re-suspension in order to remove excess sodium pyrophosphate, to eliminate larger aggregates/agglomerates and to minimize the content of free, ionic ^{48}V (see Supplementary Materials (SM-IV)). The final size selected and

radiolabeled, nano-sized aggregates or agglomerates of [^{48}V]TiO_2NP were suspended and dispersed in water.

For each of the retention time points to be studied a new batch of size-selected [^{48}V]TiO_2NP was prepared, characterized and immediately applied intravenously, by gavage or intratracheal instillation to groups of four rats each, which improves the comparability between the exposure routes as the studies were started with the same nanoparticle properties.

Characterization of [^{48}V]TiO_2NP

The hydrodynamic diameter of the size-selected [^{48}V]TiO_2NP and the zeta potential were measured in triplicates several times during the size selection process for control purposes and prior to IV-injection using a Malvern Zetasizer (Malvern, Herrenberg, Germany). Samples for transmission electron microscopy were prepared from the aqueous suspension ready for administration on glow discharged 300 mesh Formvar®-coated copper grids and investigated with a Philips 300 TEM at 60 kV acceleration voltage.

Study design – Main study with [^{48}V]TiO_2NP and auxiliary study with soluble ^{48}V

After a single IV-injection dose of typically 10-20 µg (1h, 4h, 24h) nano-sized [^{48}V]TiO_2NP suspended in 60 µL water into the tail vein over 20-30 seconds, the biokinetics was followed in five groups of four rats each up to five time points (1h, 4h, 24h, 7d and 28d) as sketched:

Study	IV-injection, 0h	dissection time-points for biodistribution analyses				
MAIN	[^{48}V]TiO_2NP	1h	4h	24h	7d	28d
AUX	^{48}V ions			24h	7d	

The time points at 7d and 28d were studied with higher doses (see Table 1) in order to ensure sufficient sensitivity in spite of radioactive decay and to detect also minor redistribution and clearing processes.

In addition to the study with [^{48}V]TiO_2NP, an auxiliary study was performed to investigate the absorption and biodistribution of soluble, ionic ^{48}V at 24h and 7d after IV-injection. These data were used for correction of ^{48}V release from the [^{48}V]TiO_2NP. In order to mimic ^{48}V released by [^{48}V]TiO_2NP we added 0.33 µg/µL ionic $Ti(NO_3)_4$ to the carrier-free, ionic ^{48}V isotope, thus obtaining a nitrate solution of sufficient ionic strength to stably maintain the ions in solution, and adjusted the pH value to 5. For the experiments 60 µL of solution containing 27 kBq ionic ^{48}V and 20 µg of ionic Ti were IV-injected into the tail vein of each rat.

Animals

Healthy, female Wistar-Kyoto (WKY) rats (Janvier, Le Genest Saint Isle, France), 8–10 weeks of age (263 ± 10 g mean (± STD) body weight) were housed in pairs in relative-humidity and temperature controlled ventilated cages on a 12-hr day/night cycle. Rodent diet and water were provided ad libitum. After purchase, the rats were adapted for at least two weeks and then randomly attributed to the experimental groups. All experiments were conducted under German federal guidelines for the use and care of laboratory animals and were approved by the Regierung von Oberbayern (Government of District of Upper Bavaria, Approval No. 211-2531-94/04) and by the Institutional Animal Care and Use Committee of Helmholtz Centre Munich.

[^{48}V]TiO_2NP IV-injection and animal maintenance in metabolic cages

Using minimal-dead-space, 1-mL-insulin-syringes (Omnican® 100, Braun, Melsungen, Germany, specified dead space <0.4µL), aqueous [^{48}V]TiO_2NP suspensions (60 µL) were intravenously injected into the tail vein of non-fasted animals early in the morning. The syringes and cannulas used for intravenous injection were collected for measurements of the residual [^{48}V]TiO_2NP content, which was motivated by the discovery of losses of nanoparticles due to adherence on the polymer syringe material. After IV-injection of the

[^{48}V]TiO_2NP suspensions, rats of the first four groups (up to 7-day retention time) were kept individually in metabolism cages for separate daily collection of urine and feces. Rats of the 28-day group were maintained individually on cotton cloths in normal cages. The cloth was replaced by a new one every 3-4 days and fecal droppings were separated from the collected cloth; after separation the dried cloth contained only non-particulate ^{48}V originating from urine.

Sample preparation and ^{48}V radioanalysis

At 1h, 4h, 24h, 7d and 28d after IV-injection, rats were anesthetized (by 5% isoflurane inhalation) and euthanized by exsanguination *via* the abdominal aorta. For γ-spectrometry, blood, all organs, tissues and excretions were collected and ^{48}V-radioactivities were measured without any further physico-chemical processing, as detailed in the SM-IV and in earlier works (Kreyling, 2011, Hirn, 2011, Kreyling, 2014, Schleh, 2012). Since by exsanguination only about 60-70% of the blood volume could be recovered the residual blood contents of organs and tissues after exsanguination were calculated according to the findings of (Oeff, 1955) and the ^{48}V-radioactivities of the organs were corrected for these contributions.

Throughout this report nanoparticle quantities are given as percentages of the total intravenously injected [^{48}V]TiO_2NP radioactivity in each animal. The total injected activity was calculated as the sum of all samples of each entire animal, including its total fecal and urinary excretion, corrected for background and radioactive decay during the experiments using detectors calibrated in γ-ray energy and detection efficiency for ^{48}V. The percentages are averaged over the group of four rats per each retention time point and are given with the standard error of the mean (SEM). Samples yielding background-corrected counts in the 511 keV region-of-interest of the ^{48}V γ-spectrum were defined to be below the detection limit (<DL; 0.2 Bq) when the number of counts was less than three standard deviations of the background counts.

The data compiled in Table 2 below are presented (i) as raw data of the ^{48}V-activity directly determined from the retrieved samples, (ii) as data corrected for the residual blood content in the organs or tissues and (iii) additionally corrected for free ^{48}V-ions. The detailed execution of these corrections is presented in the SM-IV. All calculated significances are based on the One-Way-ANOVA test and the post-hoc Tukey test. In case of direct two-groups comparison, the unpaired t-test was used. $p \leq 0.05$ was considered significant.

Results

Physicochemical properties of [^{48}V]TiO_2NP

The size distributions of the size-selected [^{48}V]TiO_2NP determined by DLS are presented in Figure 1. These were prepared for each of the five retention time points prior to intravenous injection. They indicate a good reproducibility of the size selection procedure. The Z-averages (see Table 1) are in a narrow range of 88 ± 11 nm, and the PDI values 0.18 ± 0.04 indicate that the size distributions have a rather narrow size distribution. Only the suspension for the 4h time point appeared to have a particle size somewhat smaller than the others. These conclusions are supported by TEM investigations after the size selection and dispersion process (see Figure 2) which revealed approximately spherical aggregated/agglomerated entities of roughly 50 nm in diameter, made up of smaller primary particles.

From the known activity concentration (1 MBq/mg (1h, 4h, 24h) and 2.35 MBq/mg (7d, 28d)) after proton irradiation and the determined ^{48}V-activity of the applied [^{48}V]TiO_2NP, the applied nanoparticle mass was calculated for each IV-injection as reported in Table 1. The effectively injected dose (activity) takes into account that a fraction of the activity loaded into the syringes was retained there after injection.

Biokinetics of [^{48}V]TiO_2NP in blood, whole organs and tissues

Table 2 gives a comprehensive summary of the biodistribution of intravenously injected [^{48}V]TiO_2NP at the five retention time points. For each organ or tissue the [^{48}V]TiO_2NP content is given in percent of the injected dose (ID) based on the measured ^{48}V-activity balance, referred to as *raw data*. As described earlier and elaborated in mathematical detail in the SM-IV the data were corrected for the residual blood retained in organs and tissues after exsanguination. These data are referred to as *w/o residual blood content*. In a next step the contribution of free ^{48}V-ions was also corrected for, referred to as *w/o free ^{48}V ions*, making use of the auxiliary study with ionic ^{48}V (see SM-IV for the mathematical correction

procedure). This step is advisable because ^{48}V could be released from [^{48}V]TiO_2NP even after careful washing during suspension preparation when diffusion processes bring radiolabels close to the surface of the nanoparticles or by a slow dissolution process of the nanoparticles (Vogelsberger, 2008). This correction effect would be most prominent if [^{48}V]TiO_2NP and free ^{48}V-ions had distinctly different biodistribution patterns. The fully corrected data are visualized in Figure 3 (panels A-C).

Table 2 shows that during the first hour after IV-injection more than 99% of [^{48}V]TiO_2NP were very rapidly removed from the blood. After that the [^{48}V]TiO_2NP concentration decreased slowly over the following week and then it remained approximately constant until day 28. This implies that the corrections for retained blood become rather small already after 1h.

The data show that the [^{48}V]TiO_2NP rapidly cleared from the blood were retained mainly in the liver (95.5% of ID after 4h) with only slow clearance from there over the entire observation period (88.9% of ID after 28d). Retention in the spleen was between 2.5% and 4% of ID over the entire observation period, while retention was only about 0.1% in the lungs. Accumulation in the kidneys increased slightly over the four-week period (from 0.05% to about 0.2% of ID) while retention in all other secondary organs, such as brain, heart and uterus was rather low, which is also reflected in the scatter of the data. No trend can be identified over the four-week period showing virtually constant values and no net clearance from those organs. The lowest, but still detectable, [^{48}V]TiO_2NP retention of 0.0005% was observed in the brain. The corrections for free ^{48}V-ions, which contribute well below 1% of to the total retained activity, may lead to significant reductions of the values for [^{48}V]TiO_2NP retention. However, since all input data are very small and subjected to large scatter, these corrections are also subject to large uncertainty. Nevertheless, the corrections are conservative enough to attribute a measureable radioactivity to the presence of a tiny amount of [^{48}V]TiO_2NP after 24h and 28d. Remarkably, the skeleton and to a lesser extend the soft

tissue (non-osseous tissues of the carcass including muscles, fat, skin, connective tissue, paws) exhibit a persistent [^{48}V]TiO_2NP content that amounts to nearly 1% and 0.7% of ID at 28d, respectively. The relatively high [^{48}V]TiO_2NP retention in the skeleton may be explained by reported experimental evidence (Rinderknecht, 2008) that [^{48}V]TiO_2NP are retained in the bone marrow following blood translocation into the bones and probable uptake by phagocytes and other cells like pluripotent stem cells.

[^{48}V]TiO_2NP concentrations per weight of organ or tissue

Due to their importance for toxicological comparisons, in Table 2 the percentages of injected activity assigned to [^{48}V]TiO_2NP after all corrections for residual blood content and presence of free ^{48}V, are converted into mass (ng) of nanoparticles per gram of organ or tissue. Since these data allow a straightforward comparison only for the same injected dose, the data are additionally presented as percentages of the injected dose per organ mass (%ID/g) and shown in Figure 3 (panel D-F). The effectively injected mass doses varied because a highly variable fraction of the [^{48}V]TiO_2NP loaded into the syringes for intravenous injection was retained there after application. Additionally, the study design has foreseen higher doses for the 7d and 28d studies, in order to preserve high detection sensitivity in spite of the radioactive decay during the prolonged retention times.

The highest concentrations of about 10-11 %ID•g^{-1} are determined in the liver and are about 2.5-4 %ID•g^{-1} in the spleen. Both of these stayed rather constant during the entire time period. In the lungs the concentrations were much lower at about 0.05 %ID•g^{-1} and remained rather constant over time. The concentrations in kidneys increased from 0.02 to 0.08 %ID•g^{-1} during the 28-days observation period. Fractional concentrations in the heart and uterus were below 0.01 %ID•g^{-1} throughout the observation period. No [^{48}V]TiO_2NP were detected in the brain at 1h, 4h and 7d (< DL) but a detectable concentration of 0.0006 %ID•g^{-1}was reached after

28d. This very low concentration is however notable since it is already corrected for nanoparticles retained in the residual blood of the brain and for free ^{48}V.

Urinary excretion

Figure 4 shows the fraction of ^{48}V-activity excreted daily in urine. The data sets obtained from the 7-days and the 28-days retention experiments were used. The data show that there is rapid decline of daily urinary excretion from 0.34% to 0.18% of ID during the first three days after IV-injection followed by a slower decrease towards 0.12%ID after 2 weeks before a plateau below 0.1%ID of daily urinary excretion is reached after about 20 days. For the applied estimates on ^{48}V-ion release we assumed no nanoparticulate urinary excretion as a conservative (upper) estimate of ionic ^{48}V-release, although excretion of smaller nanoparticles cannot be totally excluded. This assumption is in agreement with the work of Choi and co-workers (Choi, 2007) who suggest that renal glomerular filtration does not allow urinary nanoparticle excretion of nanoparticles larger than 8 nm.

Hepato-biliary [^{48}V]TiO_2NP clearance (HBC)

[^{48}V]TiO_2NP observed in the gastro-intestinal tract (GIT) and fecal excretions resulted from their clearance from the liver *via* bile into the small intestine. The cumulative cleared fraction of [^{48}V]TiO_2NP is shown in Figure 5. Over four weeks there was a steady increase of clearance up to about 3% of the applied dose *via* this pathway.

Discussion

In order to estimate relevant dose levels for nanoparticle toxicology studies we should consider the main routes of intake which are either *via* inhalation or ingestion, since there is growing evidence that dermal uptake is usually so low that it is not detectable (Gontier, 2008). For inhalation the New Energy and Industrial Technology Development Organization

(NEDO) in Japan has recently estimated an acceptable workplace airborne particulate concentration to be 1.2 mg/m^3 TiO_2NP as a time weighted average for an 8h working day and a 40h working week (Morimoto, 2010). This may lead to a daily deposited TiO_2NP dose in the lungs of 2.4 mg per day (assuming an inhaled volume of 20 m³ per day and a deposition fraction of 0.3 averaged over a size range of 20-100 nm (MPPD (Multiple Path Particle Dosimetry); ((A.R.A.), 2009) corresponding to a daily dose of 34 µg/kg BW for a normal 70-kg person. No human translocation data across the air-blood barrier (ABB) are available but based on animal data the daily translocated TiO_2NP fraction should be 1% or less (Kreyling, 2013). Therefore, a relevant daily dose to the circulation resulting from inhalation should not exceed 0.34 µg/kg BW.

A similar estimate can be made for ingested TiO_2NP: Based on a survey of the British population (Lomer, 2004) the average daily intake of submicron and nano-sized TiO_2 particles is 2.5 mg/d by an average consumer corresponding to a daily dose of about 35 µg/kg BW of a normal 70-kg person. Also for absorbed TiO_2NP across the human gut no consolidated data are available but based on animal data the daily absorbed TiO_2NP fraction should be 5% or less (Jani, 1990). Therefore, a realistic daily dose to the circulation resulting from ingested and absorbed TiO_2NP should not exceed 2 µg/kg BW. Taking together the daily TiO_2NP absorbed through the gut epithelium into the circulation, a relevant daily dose would be a few tenths of µg/kg BW. With respect to this value, IV-injected TiO_2NP doses of 1 mg/kg BW are 100-fold higher or more and usually applied over about 10 seconds corresponding to instantaneous dose rates about a million times higher than in realistic exposure scenarios. For the identification of potential organs at risk the extrapolation from results obtained from such high and even higher doses are not straightforward. In light of these considerations *in vivo* biokinetics studies using TiO_2NP intravenous doses beyond tenths of µg/kg BW need solid justification.

For the present study a commercially available, engineered pure titanium dioxide material with (aggregated/agglomerated) primary particles of 7-10 nm in size has been used.. In contrast to many other studies our study aim was to quantify the biokinetics fate of nanoparticles (<100nm) in the entire organism, including total excretion, by making use of the high sensitivity of radiotracer studies which are not susceptible to matrix and background effects or artefacts introduced by specimen preparation. Hence, a truly nano-sized fraction was separated and prepared for simultaneous IV-injection, gavage and intratracheal instillation. The preparation was repeated five times to study a single retention time point (1h, 4h, 24, 7 days and 28 days) by all three exposure routes with the same [^{48}V]TiO_2NP suspension. Quantitative biokinetics studies analyzing the entire organism with similar precision are presently not available in literature. However, several papers have also reported highest particle accumulations in the liver, followed by spleen, and then by the other organs studied (Fabian, 2008, Geraets, 2014, Louro, 2014, Patri, 2009, Shi, 2013, Yamashita, 2011) (Xie, 2011). In addition, there is a recent review on the toxicology of titanium dioxide nanoparticle including a discussion of biokinetics (Shi, 2013), but no data are reported concerning nanoparticle translocation to the skeleton and soft tissues.

Using ^{48}V-labeled pure anatase TiO_2NP allowed us to perform rather precise determinations of the biokinetics of IV-injected [^{48}V]TiO_2NP over a dynamic dose range of five orders of magnitude between the applied dose and the content in individual organs and tissues up to 28 days after IV-injection. Since we found that blood contained circulating [^{48}V]TiO_2NP at any retention time, we estimated the [^{48}V]TiO_2NP content in the residual blood volume of each organ and tissue after exsanguination by applying the results of Oeff and Konig (Oeff, 1955), and subtracted this amount from the measured organ activity to determine with greater accuracy the parenchymal [^{48}V]TiO_2NP organ/tissue content.

Additionally, we aimed to use rather low [^{48}V]TiO_2NP doses of about 10 µg/rat for the biokinetics studies up to 24 hours and of about 100 µg/rat for the 7-day and 28-day studies (to

compensate for radioactive ^{48}V decay and [^{48}V]TiO_2NP elimination from the body), which is a compromise between physiologically reasonable daily doses and preserving high detection sensitivity. The combination of applied low doses and high detection sensitivity ensures that, neither the rather low [^{48}V]TiO_2NP mass used in our study nor its radioactivity is likely to cause any detectable detrimental effect. Additionally, the ^{48}V-radioactivity concentration chosen corresponded to an atomic ratio of ^{48}V:Ti in the order of 4×10^{-7} which represents a negligible mass-impurity of the ^{48}V in the TiO_2NP matrix, unlikely to affect its lattice stability or any physico-chemical property.

However, the study design is also associated with some shortcomings. This study remains at the level of macroscopic biokinetics and does not provide any microscopic details, such as any cell-type interactions with the [^{48}V]TiO_2NP in any of the secondary organs or tissues, which of course would have been highly desirable. It should be noted that we never directly observed actual TiO_2 particles in our *in vivo* studies and relied on γ-spectrometric determination of ^{48}V-activity. At the low activity levels detected in some organs the calculated amounts of [^{48}V]TiO_2NP are more sensitive to errors especially when subtracting the estimated contribution of free ^{48}V-ions. Therefore, further independent studies with similarly high sensitivity are desirable. Although we corrected for the [^{48}V]TiO_2NP content in the residual blood of all organs and tissues, we could not distinguish between [^{48}V]TiO_2NP content translocated to the parenchyma and that eventually trapped in the walls of minor blood vessels. Yet, at the doses chosen it would have been impossible to identify and quantify [^{48}V]TiO_2NP in biological specimens using electron microscopy because of their very sparse distribution in any of the secondary organs and tissues probably with exception of the liver. However, in a previous inhalation study on WKY rats using freshly generated TiO_2 anatase nanoparticles (median size 20 nm) the lung distribution of TiO_2NP had been morphometrically quantified by TEM analysis (Geiser, 2008, Geiser, 2005). Furthermore, in an earlier study, we have identified 18 nm gold nanoparticles in electron-micrographs of

Kupffer cells, hepatocytes and endothelial cells of the rat liver 24h after IV-injection (Hirn, 2011), indicating that nanoparticles do indeed translocate into the organ tissues.

Intravenous injection of suspended [^{48}V]TiO_2NP provides a high dose rate to blood. Therefore, it is likely that only very few nanoparticles will be taken up by monocytes and/or thrombocytes of the blood and, hence, most will initially interact and bind to blood proteins and biomolecules (called opsonization or more recently protein-corona) which subsequently will affect uptake in organs and tissues. Most organs and tissues have only a relatively low capacity for acute particle uptake via their mononucleated-phagocytic-system (MPS) which differs considerably between organs and tissues (Hume, 2008). In contrast, the liver has a high capacity which causes rapid and predominant accumulation in the liver for many nanoparticles (Almeida, 2011, Zarschler, 2016). This uptake is likely be affected by the protein-corona in blood. However, it remains unclear which biomolecules lead to rapid receptor recognition and phagocytosis by Kupffer cells, and, likewise, how and by which biomolcule mediation the uptake occurs in MPS cells of the other organs and tissues. After only 1h the [^{48}V]TiO_2NP concentration in blood decreases 200-fold so that circulating [^{48}V]TiO_2NP may well be phagocytized/endocytosed, and subsequently the composition of the dynamic protein corona may change and/or blood monocytes and thrombocytes may modify their further fate in the body.

It is quite remarkable how constant the [^{48}V]TiO_2NP retention is in most of the organs, skeleton and the tissue after the correction for ^{48}V release from the nanoparticle matrix (see Table 2 and Figure 3). It underlines the stability of the nano-fraction of the commercial ST-01 TiO_2 powder and its radiolabel ^{48}V. However, the increasing hepato-biliary clearance (HBC) over time (see Figure 5) highlights that minor biokinetic [^{48}V]TiO_2NP exchanges and/or clearance occurs in the liver and probably in the entire organism over time. The cumulative HBC steadily increases up to 3% over 28 days. In our previous IV-injection study we could only determine 24-hour data because of the short half-life of the ^{198}Au radiotracer used, but

we showed that HBC is linearly inversely related to the Au nanoparticles diameter between 2.8 nm to 80 nm (Hirn, 2011). For 80-nm-size Au nanoparticles we obtained 0.5% HBC after 24h. This corresponds reasonably well with the clearance level of 70 nm [^{48}V]TiO_2NP (0.4%) at 24h found in this study. Differences may be related to the differences in nanoparticle materials and/or their morphologies.

In the SM-IV (Figure S7) we derive a small release rate (less than 0.1% per day) of ^{48}V from the [^{48}V]TiO_2NP which appears to be effective during the whole study period of 28d. This might be interpreted either as loss of imperfectly fixed labels in the TiO_2 matrix or as a very slow dissolution and shrinking of the nanoparticles (Vogelsberger, 2008) setting free less than 0.1% of the nanoparticle mass per day. If the latter would be the case (or even a combination of the two) such a process may contribute to nanoparticle clearance from organs and from the organism.

Conclusion

The quantitatively balanced biokinetics assay used for retention times up to 28d after IV-injection of ^{48}V radiolabeled TiO_2NP provides a sensitive methodology with a dynamic dose range over five orders of magnitude and allows quantitative [^{48}V]TiO_2NP distribution balancing at each retention time point in the entire organism, including excretions. The ^{48}V release rate from the [^{48}V]TiO_2NP matrix was less than 0.1% per day and the ^{48}V-activity related to free ^{48}V-ions was corrected for according to the auxiliary biokinetics study on ionic ^{48}V. [^{48}V]TiO_2NP were detected in most organs and tissues most likely retained in their MPS. Highest [^{48}V]TiO_2NP accumulations were found in liver (95.5% ID during day-1), followed by spleen (2.3%), skeleton (0.7%), blood (0.5%) and, with detectable nanoparticle burdens in all other organs. It is remarkable that nanoparticles were retained in organs and tissues that are usually not considered in biodistribution studies. The [^{48}V]TiO_2NP content in blood decreased 200-fold within one hour while the distribution in other organs and tissues remained roughly

constant over 28 days. Hepato-biliary clearance of [^{48}V]TiO_2NP from the liver continued over the entire 28-days period.

Acknowledgements

We would like to thank Sebastian Kaidel, Paula Mayer and Nadine Senger from the Helmholtz Center Munich for their excellent technical assistance, as well as Antonio Bulgheroni, Kamel Abbas, Federica Simonelli, Izabela Cydzik and Giulio Cotogno from the EU-Joint Research Center who strongly supported the nanoparticle radiolabeling activities. We also express our sincere gratitude to Barbara Rothen-Rutishauser and David Raemy from the University of Fribourg, Switzerland, who performed the TEM analysis of the TiO_2NP.

Declaration of Interest

The authors declare that they have no financial, consulting, and personal relationships with other people or organizations that could influence (bias) the author's work.

This work was partially supported by the German Research Foundation SPP 1313, the EU-FP6 project Particle-Risk (012912 (NEST)), and the EU FP7 projects NeuroNano (NMP4-SL-2008-214547), ENPRA (NMP4-SL-2009-228789) and InLiveTox (NMP-2008-1.3-2 CP-FP 228625-2).

Supplementary Material available online.

- Radiolabeling of titanium dioxide (TiO_2) nanoparticles
- Nanoparticle preparation for application and characterization
- Animals and animal housing
- Nanoparticle application and animal maintenance in metabolic cages
- Sample preparation for radiometric analysis
- Radiometric and statistical analysis
- Blood correction and total blood volume

- ^{48}V-activity determination of skeleton and soft tissue
- Biokinetics of soluble ^{48}V in ionic form after IV-injection
- Correction of the biokinetics assigned to [^{48}V]TiO_2NP for the effect of free ^{48}V-ions
- Evaluation of the auxiliary and main study by pharmacokinetic modeling

References

(A.R.A.), ARA 2009. Multiple-path particle dosimetry model (MPPD version 3.0).

Almeida, JPM, Chen, AL, Foster, A & Drezek, R 2011. In vivo biodistribution of nanoparticles. *Nanomedicine,* 6**,** 815-835.

Auttachoat, W, McLoughlin, CE, White, KL, Jr. & Smith, MJ 2013. Route-dependent systemic and local immune effects following exposure to solutions prepared from titanium dioxide nanoparticles. *J Immunotoxicol*.

Carlander, U, Li, D, Jolliet, O, Emond, C & Johanson, G 2016. Toward a general physiologically-based pharmacokinetic model for intravenously injected nanoparticles. *Intrnational Journal of Nanomedicine,* 11**,** 625-640.

Choi, HS, Liu, W, Misra, P, Tanaka, E, Zimmer, JP, Ipe, BI, Bawendi, MG & Frangioni, JV 2007. Renal clearance of quantum dots. *Nature Biotechnology,* 25**,** 1165-1170.

Christensen, FM, Johnston, HJ, Stone, V, Aitken, RJ, Hankin, S, Peters, S & Aschberger, K 2011. Nano-TiO(2) - feasibility and challenges for human health risk assessment based on open literature. *Nanotoxicology,* 5**,** 110-24.

Fabian, E, Landsiedel, R, Ma-Hock, L, Wiench, K, Wohlleben, W & Van Ravenzwaay, B 2008. Tissue distribution and toxicity of intravenously administered titanium dioxide nanoparticles in rats. *Archives of Toxicology,* 82**,** 151-7.

Geiser, M, Casaulta, M, Kupferschmid, B, Schulz, H, Semmler-Behnke, M & Kreyling, W 2008. The role of macrophages in the clearance of inhaled ultrafine titanium dioxide particles. *American Journal of Respiratory Cell and Molecular Biology,* 38**,** 371-6.

Geiser, M, Rothen-Rutishauser, B, Kapp, N, Schurch, S, Kreyling, W, Schulz, H, Semmler, M, Im Hof, V, Heyder, J & Gehr, P 2005. Ultrafine particles cross cellular membranes by nonphagocytic mechanisms in lungs and in cultured cells. *Environmental Health Perspectives,* 113**,** 1555-60.

Geraets, L, Oomen, AG, Krystek, P, Jacobsen, NR, Wallin, H, Laurentie, M, Verharen, HW, Brandon, EF & De Jong, WH 2014. Tissue distribution and elimination after oral and intravenous administration of different titanium dioxide nanoparticles in rats. *Part Fibre Toxicol,* 11**,** 30.

Gontier, E, Ynsa, M-D, Bíró, T, Hunyadi, J, Kiss, B, Gáspár, K, Pinheiro, T, Silva, J-N, Filipe, P, Stachura, J, Dabros, W, Reinert, T, Butz, T, Moretto, P & Surlève-Bazeille, J-E 2008. Is there penetration of titania nanoparticles in sunscreens through skin? A comparative electron and ion microscopy study. *Nanotoxicology,* 2**,** 218-231.

Gu, Z, Rolfe, BE, Thomas, AC & Xu, ZP 2013. Restenosis treatments using nanoparticle-based drug delivery systems. *Curr Pharm Des,* 19**,** 6330-9.

Hirn, S, Semmler-Behnke, M, Schleh, C, Wenk, A, Lipka, J, Schaffler, M, Takenaka, S, Moller, W, Schmid, G, Simon, U & Kreyling, WG 2011. Particle size-dependent and surface charge-dependent biodistribution of gold nanoparticles after intravenous administration. *European Journal of Pharmaceutics and Biopharmaceutics,* 77**,** 407-16.

Hume, DA 2008. Differentiation and heterogeneity in the mononuclear phagocyte system. *Mucosal Immunol,* 1**,** 432-41.

Jani, P, Halbert, GW, Langridge, J & Florence, AT 1990. Nanoparticle uptake by the rat gastrointestinal mucosa: quantitation and particle size dependency. *J Pharm Pharmacol,* 42**,** 821-6.

Jia, L, Xu, M, Zhen, W, Shen, X, Zhu, Y, Wang, W & Wang, X 2008. Novel anti-oxidative role of calreticulin in protecting A549 human type II alveolar epithelial cells against hypoxic injury. *Am J Physiol Cell Physiol,* 294**,** C47-55.

Kreyling, WG, Biswas, P, Messing, ME, Gibson, N, Geiser, M, Wenk, A, Sahu, M, Deppert, K, Cydzik, I, Wigge, C, Schmid, O & Semmler-Behnke, M 2011. Generation and

characterization of stable, highly concentrated titanium dioxide nanoparticle aerosols for rodent inhalation studies. *Journal of Nanoparticle Research,* 13**,** 511–524.

Kreyling, WG, Hirn, S, Moller, W, Schleh, C, Wenk, A, Celik, G, Lipka, J, Schaffler, M, Haberl, N, Johnston, BD, Sperling, R, Schmid, G, Simon, U, Parak, WJ & Semmler-Behnke, M 2014. Air-blood barrier translocation of tracheally instilled gold nanoparticles inversely depends on particle size. *ACS Nano,* 8**,** 222-33.

Kreyling, WG, Holzwarth, U, Haberl, N, Kozempel, J, Wenk, A, Hirn, S, Schleh, C, Schäffler, M, Lipka, J, Semmler-Behnke, M & Gibson, N submitted-a. Part 3: Quantitative biokinetics of titanium dioxide nanoparticles after intratracheal instillation in rats. *Nanotoxicology***,** (submitted).

Kreyling, WG, Holzwarth, U, Schleh, C, Kozempel, J, Wenk, A, Haberl, N, Hirn, S, Schäffler, M, Lipka, J, Semmler-Behnke, M & Gibson, N submitted-b. Part 2: Quantitative biokinetics of titanium dioxide nanoparticles after oral application in rats *Nanotoxicology***,** (submitted).

Kreyling, WG, Semmler-Behnke, M, Takenaka, S & Moller, W 2013. Differences in the biokinetics of inhaled nano- versus micrometer-sized particles. *Acc Chem Res,* 46**,** 714-22.

Kreyling, WG, Semmler, M, Erbe, F, Mayer, P, Takenaka, S, Schulz, H, Oberdörster, G & Ziesenis, A 2002. Translocation of ultrafine insoluble iridium particles from lung epithelium to extrapulmonary organs is size dependent but very low. *Journal of Toxicology and Environmental Health-Part A,* 65**,** 1513-1530.

Li, N, Xia, T & Nel, AE 2008. The role of oxidative stress in ambient particulate matter-induced lung diseases and its implications in the toxicity of engineered nanoparticles. *Free Radic.Biol Med,* 44**,** 1689-1699.

Lomer, MC, Hutchinson, C, Volkert, S, Greenfield, SM, Catterall, A, Thompson, RP & Powell, JJ 2004. Dietary sources of inorganic microparticles and their intake in healthy subjects and patients with Crohn's disease. *British Journal of Nutrition,* 92**,** 947-55.

Louro, H, Tavares, A, Vital, N, Costa, PM, Alverca, E, Zwart, E, De Jong, WH, Fessard, V, Lavinha, J & Silva, MJ 2014. Integrated approach to the in vivo genotoxic effects of a titanium dioxide nanomaterial using LacZ plasmid-based transgenic mice. *Environ Mol Mutagen,* 55**,** 500-9.

Matusiewicz, H 2014. Potential release of in vivo trace metals from metallic medical implants in the human body: from ions to nanoparticles--a systematic analytical review. *Acta Biomater,* 10**,** 2379-403.

Morimoto, Y, Kobayashi, N, Shinohara, N, Myojo, T, Tanaka, I & Nakanishi, J 2010. Hazard assessments of manufactured nanomaterials. *J Occup Health,* 52**,** 325-34.

Ninomiya, K, Fukuda, A, Ogino, C & Shimizu, N 2014. Targeted sonocatalytic cancer cell injury using avidin-conjugated titanium dioxide nanoparticles. *Ultrason Sonochem,* 21**,** 1624-8.

Oeff, K & Konig, A 1955. [Blood volume of rat organs and residual amount of blood after blood letting or irrigation; determination with radiophosphorus-labeled erythrocytes.]. *Naunyn-Schmiedebergs Archiv für Experimentelle Pathologie und Pharmakologie,* 226**,** 98-102.

Patri, A, Umbreit, T, Zheng, J, Nagashima, K, Goering, P, Francke-Carroll, S, Gordon, E, Weaver, J, Miller, T, Sadrieh, N, McNeil, S & Stratmeyer, M 2009. Energy dispersive X-ray analysis of titanium dioxide nanoparticle distribution after intravenous and subcutaneous injection in mice. *Journal of Applied Toxicology,* 29**,** 662-672.

Peters, RJ, Van Bemmel, G, Herrera-Rivera, Z, Helsper, JP, Marvin, HJ, Weigel, S, Tromp, P, Oomen, AG, Rietveld, A & Bouwmeester, H 2014. Characterisation of titanium

dioxide nanoparticles in food products: Analytical methods to define nanoparticles. *J Agric Food Chem*.

Rinderknecht, A, Prudhomme, R, Poreda, R, Gelein, R, Corson, N, Pidruczny, A, Finkelstein, J, Oberdorster, G & Elder, A 2008. Biokinetics of Au nanoparticles relative to size surface coating and portal of entry. *47th Annual Society of Toxicology Meeting; Seattle, WA*.

Sadauskas, E, Danscher, G, Stoltenberg, M, Vogel, U, Larsen, A & Wallin, H 2009. Protracted elimination of gold nanoparticles from mouse liver. *Nanomedicine,* 5**,** 162-9.

Schleh, C, Semmler-Behnke, M, Lipka, J, Wenk, A, Hirn, S, Schaffler, M, Schmid, G, Simon, U & Kreyling, WG 2012. Size and surface charge of gold nanoparticles determine absorption across intestinal barriers and accumulation in secondary target organs after oral administration. *Nanotoxicology,* 6**,** 36-46.

Semmler-Behnke, M, Takenaka, S, Fertsch, S, Wenk, A, Seitz, J, Mayer, P, Oberdörster, G & Kreyling, WG 2007. Efficient elimination of inhaled nanoparticles from the alveolar region: evidence for interstitial uptake and subsequent reentrainment onto airways epithelium. *Environmental Health Perspectives,* 115**,** 728-33.

Semmler, M, Seitz, J, Erbe, F, Mayer, P, Heyder, J, Oberdörster, G & Kreyling, WG 2004. Long-term clearance kinetics of inhaled ultrafine insoluble iridium particles from the rat lung, including transient translocation into secondary organs. *Inhalation Toxicology,* 16**,** 453-9.

Setyawati, MI, Tay, CY, Chia, SL, Goh, SL, Fang, W, Neo, MJ, Chong, HC, Tan, SM, Loo, SC, Ng, KW, Xie, JP, Ong, CN, Tan, NS & Leong, DT 2013. Titanium dioxide nanomaterials cause endothelial cell leakiness by disrupting the homophilic interaction of VE-cadherin. *Nat Commun,* 4**,** 1673.

Shi, H, Magaye, R, Castranova, V & Zhao, J 2013. Titanium dioxide nanoparticles: a review of current toxicological data. *Part Fibre Toxicol,* 10**,** 15.

Vogelsberger, W, Schmidt, J., Roelfs, F. 2008. Dissolution kinetics of oxide nanoparticles: The observation of an unusual behaviour. . *Colloids and Surfaces A,* 324**,** 51-57.

Wang, T, Jiang, H, Wan, L, Zhao, Q, Jiang, T, Wang, B & Wang, S 2015. Potential application of functional porous TiO2 nanoparticles in light-controlled drug release and targeted drug delivery. *Acta Biomater,* 13**,** 354-63.

Weir, A, Westerhoff, P, Fabricius, L, Hristovski, K & Von Goetz, N 2012. Titanium dioxide nanoparticles in food and personal care products. *Environmental Science & Technology,* 46**,** 2242-50.

Xie, GP, Wang, C, Sun, J & Zhong, GR 2011. Tissue distribution and excretion of intravenously administered titanium dioxide nanoparticles. *Toxicology Letters,* 205**,** 55-61.

Yamashita, K, Yoshioka, Y, Higashisaka, K, Mimura, K, Morishita, Y, Nozaki, M, Yoshida, T, Ogura, T, Nabeshi, H, Nagano, K, Abe, Y, Kamada, H, Monobe, Y, Imazawa, T, Aoshima, H, Shishido, K, Kawai, Y, Mayumi, T, Tsunoda, S, Itoh, N, Yoshikawa, T, Yanagihara, I, Saito, S & Tsutsumi, Y 2011. Silica and titanium dioxide nanoparticles cause pregnancy complications in mice. *Nature Nanotechnology,* 6**,** 321-8.

Zarschler, K, Rocks, L, Licciardello, N, Boselli, L, Polo, E, Garcia, KP, De Cola, L, Stephan, H & Dawson, KA 2016. Ultrasmall inorganic nanoparticles: State-of-the-art and perspectives for biomedical applications. *Nanomedicine,* 12**,** 1663-701.

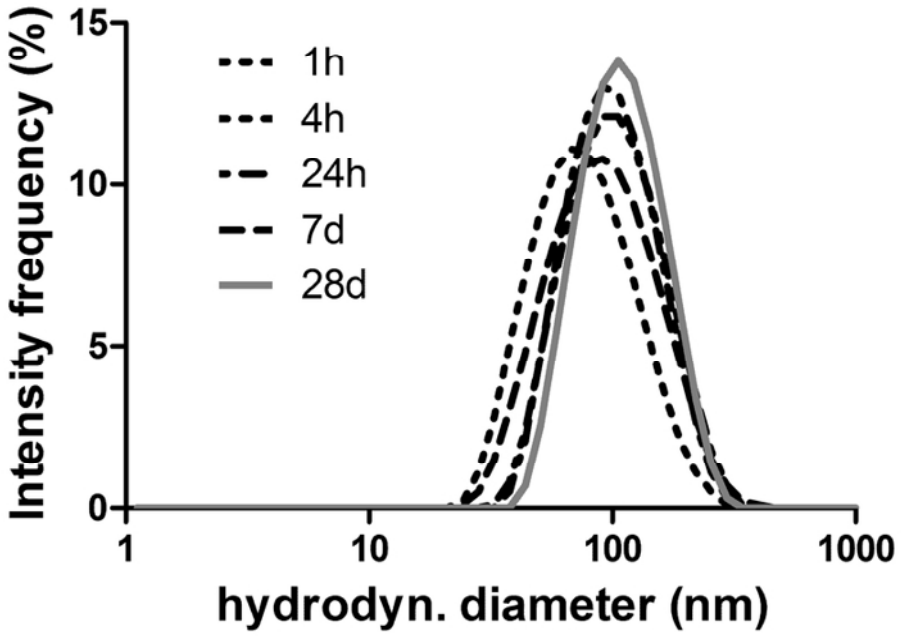

Figure 1: Hydrodynamic diameter of the five separately prepared [48V]TiO2NP suspensions used to study the five retention times of 1h, 4h, 24h, 7d and 28d measured directly before IV-injection.

73x52mm (300 x 300 DPI)

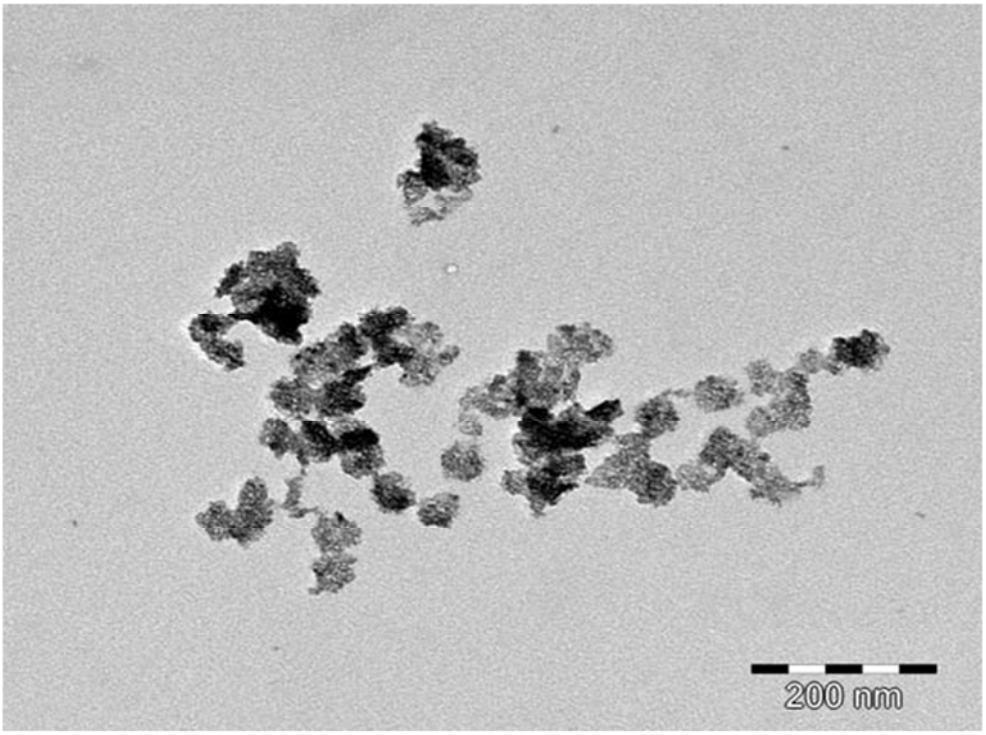

Figure 2: Transmission electron micrograph of size-selected TiO2NP sampled immediately after the size-selection procedure. TEM sample preparation leads to 'clumping' together of aggregates/agglomerates on the support grid.

254x190mm (96 x 96 DPI)

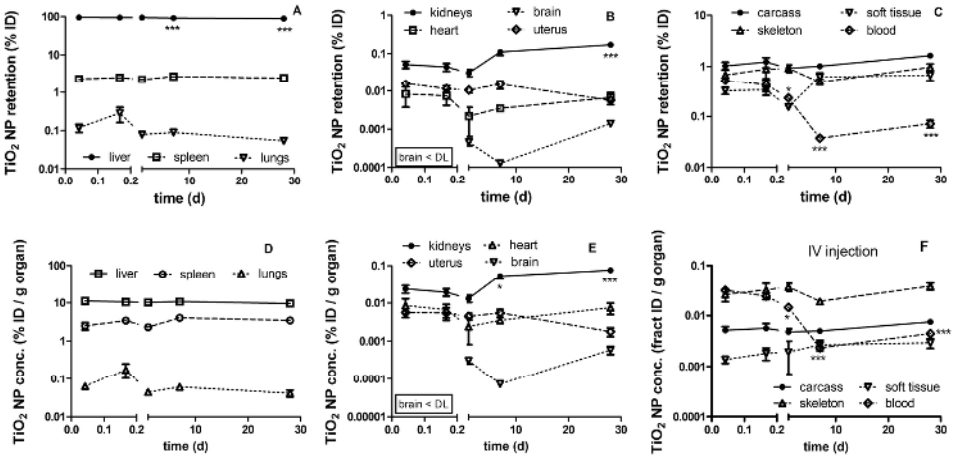

Figure 3: Graphical presentation of the biokinetics of IV-injected [48V]TiO2NP. The [48V]TiO2NP retention is expressed in terms of the retained percentage of the effectively injected nanoparticle dose which is equivalent to the percentage of injected 48V-activity corrected for the effect of free 48V-ions (% ID) (panels A-C). In panels D-F the values normalized to the organ weight are presented in %ID•g-1. Mean ± SEM of n=4 rats at each time point. Compared to 1h data levels of significance are $p<0.05$ (*), $p<0.01$ (**), $p<0.001$ (***).

141x69mm (300 x 300 DPI)

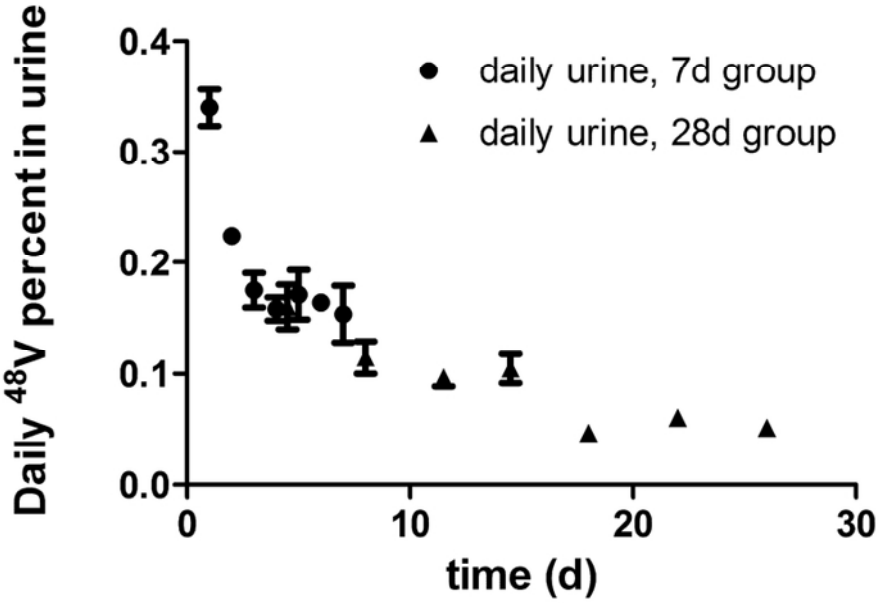

Figure 4: Daily urinary 48V-activity excretion presented as percent-rates of the total IV-injected radioactivity (%ID) over four weeks. Data from 24h to 7d after IV-injection are daily averages of the 24h group and the 7d group (n = 4). Data of the 28d group were determined as integral samples over 3-4 days and are plotted as daily urinary excretion at the mean day of the sampling period. Mean ± SEM of n=4 rats at each time point.

75x49mm (300 x 300 DPI)

Figure 5, IV, 13-12-2016

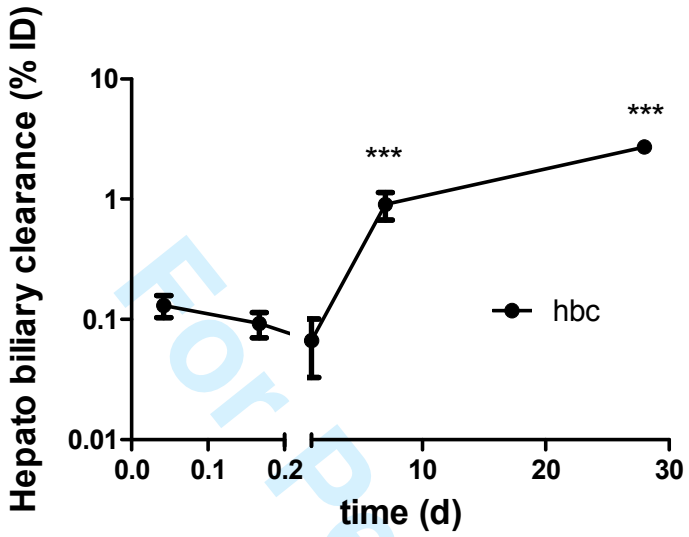

Figure 5: Cumulative Hepato-Biliary Clearance (HBC) of [^{48}V]TiO_2NP from the liver into the GIT and fecal excretions as percent of the total IV-injected [^{48}V]TiO_2NP radioactivity (%ID) over four weeks. Mean ± SEM of n=4 rats at each time point. Compared to 1h data levels of significance are $p<0.001$ (***).

Table 1: Physicochemical characteristics of the [^{48}V]TiO_2NP suspensions used for IV-injection studies at five different retention times and the mean values of the applied ^{48}V activity and mass of [^{48}V]TiO_2NP effectively received by the rats. The mean dose in µg/kg BW is also given. Additionally, [^{48}V]TiO_2NP losses in the syringe and/or cannula are provided as detailed in SI-IV.

Retention time		1h	4h	24h	7d	28d
Zeta Potential	[mV]	-38.9 ± 4.2	-33.2 ± 2.4	-29.9 ± 8.1	-42.7 ± 9.2	-35.2 ± 7.6
Z-average	[nm]	93	72	93	82	101
PDI		0.157	0.228	0.160	0.197	0.135
Effective ^{48}V radioactivity received by rats	[kBq]	18.15 ± 3.37	11.29 ± 3.69	16.53 ± 3.69	253.99 ± 54.23	110.27 ± 5.76
applied [^{48}V]TiO_2NP mass	[µg]	18.15 ± 3.37	11.29 ± 3.69	16.53 ± 3.69	108.08 ± 54.23	23.08 ± 46.92
Mean applied dose	[µg/g BW]	69.62 ± 69.7	40.13 ± 13.29	60.24 ± 13.29	392.54 ± 73.52	127.44 ± 10.17
Percentage of [^{48}V]TiO_2NP retained in the syringe after application	[%]	62.8 ± 6.2	71.3 ± 1.7	32.6 ± 4.5	n.d.	n.d.

Table 2: [^{48}V]TiO_2NP retention in organs and tissues at five time points 1h, 4 h, 24h, 7d and 28d after intravenous injection. The data are presented as retained percentage of the total intravenously injected [^{48}V]TiO_2NP dose (*raw data*). The raw data were corrected for the [^{48}V]TiO_2NP content in the residual blood present in organs and tissues after exsanguination (*w/o residual blood content*) and additionally for the contributions of free ^{48}V-ions to the biodistribution (*w/o free ^{48}V*). After these corrections the ^{48}V-activity data were converted into [^{48}V]TiO_2NP concentrations per mass of organ or tissue, given in ng·g^{-1}, and as %ID·g^{-1}. Since the effectively applied [^{48}V]TiO_2NP doses varied due to nanoparticle retention in the syringes and were intentionally increased for the 7d and 28d groups most mass concentrations in ng·g^{-1} exhibit an increase from 24h to 7d. The values in %ID·g^{-1} are independent of the applied doses. (< DL = below detection limit).

	retention time (d)	1h	4h	24h	7d	28d
organ	percent (%)	mean ± SEM	mean ± SEM	mean ± SEM	mean ± SEM	mean ± SEM
liver	raw data (% ID)	95.56 ± 0.42	94.77 ± 0.50	94.61 ± 0.23	92.55 ± 0. 50	88.97 ± 0.17
liver	w/o resid. blood cont.	95.52 ± 0.42	94.74 ± 0.51	94.59 ± 0.23	92.54 ± 0.50	88.96 ± 0.17
liver	w/o free 48V	95.50 ± 0.42	94.70 ± 0.51	94.48 ± 0.23	92.44 ± 0.45	88.92 ± 0.17
liver	TiO_2 conc. (% ID·g^{-1} tiss.)	11.14 ± 0.19	10.62 ± 0.23	10.16 ± 0.18	10.74 ± 0.32	9.67 ± 0.62
liver	TiO_2 conc. (ng·g^{-1} tiss.)	2008 ± 222	1208 ± 213	1682 ± 38	11564 ± 1243	4551 ± 364
spleen	raw data (% ID)	2.35 ± 0.26	2.57 ± 0.18	2.27 ± 0.07	2.77 ± 0.20	2.48 ± 0.27
spleen	w/o resid. blood cont.	2.35 ± 0.2576	2.57 ± 0.18	2.27 ± 0.07	2.77 ± 0.20	2.48 ± 0.27
spleen	w/o free 48V	2.34 ± 0.26	2.57 ± 0.18	2.26 ± 0.07	2.75 ± 0.20	2.48 ± 0.27
spleen	TiO_2 conc. (% ID·g^{-1} tiss.)	2.51 ± 0.55	3.43 ± 0.31	2.32 ± 0.21	4.06 ± 0.44	3.49 ± 0.32
spleen	TiO_2 conc. (ng·g^{-1} tiss.)	454 ± 122	402 ± 90	384 ± 35	4299 ± 389	1635 ± 145
kidneys	raw data (% ID)	0.078 ± 0.011	0.078 ± 0.018	0.100 ± 0.007	0.169 ± 0.018	0.193 ± 0.012
kidneys	w/o resid. blood cont.	0.062 ± 0.010	0.065 ± 0.015	0.090 ± 0.007	0.167 ± 0.018	0.191 ± 0.012
kidneys	w/o free 48V	0.0523± 0.0111	0.045 ± 0.0107	0.032 ± 0.007	0.112 ± 0.021	0.172 ± 0.011
kidneys	TiO_2 conc. (% ID·g^{-1} tiss.)	0.023 ± 0.005	0.019 ± 0.004	0.0131 ± 0.003	0.053 ± 0.010	0.076 ± 0.007
kidneys	TiO_2 conc. (ng·g^{-1} tiss.)	3.89 ± 0.43	1.93 ± 0.15	2.16 ± 0.44	54.10 ± 6.05	35.60 ± 2.39
lungs	raw data (% ID)	0.134 ± 0.032	0.297 ± 0.125	0.092 ± 0.010	0.095 ± 0.013	0.057 ± 0.008
lungs	w/o resid. blood cont.	0.119 ± 0.028	0.286 ± 0.123	0.083 ± 0.009	0.094 ± 0.013	0.055 ± 0.008
lungs	w/o free 48V	0.118 ± 0.029	0.285 ± 0.123	0.079 ± 0.009	0.089 ± 0.013	0.054 ± 0.008
lungs	TiO_2 conc. (% ID·g^{-1} tiss.)	0.063 ± 0.008	0.178 ± 0.0742	0.044 ± 0.005	0.060 ± 0.009	0.041 ± 0.008
lungs	TiO_2 conc. (ng·g^{-1} tiss.)	10.83 ± 0.43	16.21 ± 3.71	7.24 ± 16.46	67.02 ± 16.46	19.51 ± 4.31
heart	raw data (% ID)	0.013 ± 0.005	0.012 ± 0.005	0.006 ± 0.001	0.005 ± 0.0002	0.008 ± 0.003
heart	w/o resid. blood cont.	0.009 ± 0.005	0.008 ± 0.003	0.004 ± 0.002	0.005 ± 0.0002	0.007 ± 0.002

heart	w/o free 48V	0.008 ± 0.005	0.007 ± 0.003	0.002 ± 0.002	0.004 ± 0.0003	0.007 ± 0.002
heart	TiO_2 conc. (% ID·g^{-1} tiss.)	0.009 ± 0.004	0.007 ± 0.003	0.002 ± 0.002	0.004 ± 0.0002	0.008 ± 0.003
heart	TiO_2 conc. (ng·g^{-1} tiss.)	1.29 ± 0.51	0.614 ± 0.111	0.40 ± 0.27	3.76 ± 0.36	3.52 ± 1.18
brain	raw data (% ID)	< DL	< DL	0.0015 ± 0.0001	0.0005 ± 0.00005	0.0015 ± 0.0002
brain	w/o resid. blood cont.	< DL	< DL	0.0009 ± 0.0001	0.0005 ± 0.00004	0.0013 ± 0.0002
brain	w/o free 48V	< DL	< DL	0.0005 ± 0.0001	< DL	0.0011 ± 0.0002
brain	TiO_2 conc. (% ID·g^{-1} tiss.)	< DL	< DL	0.0003 ± 0.0001	< DL	0.0006 ± 0.0001
brain	TiO_2 conc. (ng·g^{-1} tiss.)	< DL	< DL	0.051 ± 0.009	< DL	0.273 ± 0.059
uterus	raw data (% ID)	0.018 ± 0.001	0.015 ± 0.003	0.016 ± 0.002	0.026 ± 0.005	0.009 ± 0.0006
uterus	w/o resid. blood cont.	0.016 ± 0.001	0.013 ± 0.003	0.015 ± 0.002	0.026 ± 0.005	0.009 ± 0.0006
uterus	w/o free 48V	0.016 ± 0.001	0.011 ± 0.002	0.011 ± 0.002	0.015 ± 0.004	0.006 ± 0.0008
uterus	TiO_2 conc. (% ID·g^{-1} tiss.)	0.006 ± 0.001	0.006 ± 0.002	0.005 ± 0.001	0.006 ± 0.001	0.002 ± 0.0005
uterus	TiO_2 conc. (ng·g^{-1} tiss.)	1.00 ± 0.15	0.66 ± 0.28	0.74 ± 0.15	5.51 ± 1.13	1.01 ± 0.15
blood	raw data (% ID)	0.524 ± 0.060	0.443 ± 0.115	0.300 ± 0.018	0.047 ± 0.004	0.075 ± 0.013
blood	w/o resid. blood cont.	0.524 ± 0.060	0.443 ± 0.115	0.300 ± 0.018	0.047 ± 0.004	0.075 ± 0.013
blood	w/o free 48V	0.512 ± 0.062	0.419 ± 0.111	0.230 ± 0.018	0.037 ± 0.003	0.072 ± 0.013
blood	TiO_2 conc. (% ID·g^{-1} tiss.)	0.031 ± 0.004	0.024 ± 0.006	0.015 ± 0.001	0.002 ± 0.0002	0.004 ± 0.0007
blood	TiO_2 conc. (ng·g^{-1} tiss.)	5.42 ± 0.10	3.60 ± 0.41	2.4006 0.19	2.48 ± 0.24	2.09 ± 0.36
carcass	raw data (% ID)	1.2 ± 0.16	1.53 ± 0.31	1.63 ± 0.12	1.75 ± 0.09	1.90 ± 0.02
carcass	w/o resid. blood cont.	1.14 ± 0.15	1.44 ± 0.23	1.57 ± 0.12	1.74 ± 0.09	1.89 ± 0.021
carcass	w/o free 48V	1.03 ± 0.18	1.22 ± 0.27	0.92 ± 0.13	1.01 ± 0.12	1.63 ± 0.03
carcass	TiO_2 conc. (% ID·g^{-1} tiss.)	0.005 ± 0.001	0.006 ± 0.001	0.005 ± 0.001	0.005 ± 0.0006	0.008 ± 0.0003
carcass	TiO_2 conc. (ng·g^{-1} tiss.)	0.89 ± 0.10	0.58 ± 0.08	0.13 ± 0.13	5.22 ± 0.23	3.54 ± 0.18
skeleton	raw data (% ID)	0.81 ± 0.13	1.02 ± 0.34	1.28 ± 0.17	1.04 ± 0.12	1.22 ± 0.16
skeleton	w/o resid. blood cont.	0.79 ± 0.13	1.00 ± 0.33	1.27 ± 0.17	1.04 ± 0.12	1.22 ± 0.16
skeleton	w/o free 48V	0.68 ± 0.16	0.88 ± 0.32	0.92 ± 0.16	0.49 ± 0.06	0.96 ± 0.15
skeleton	TiO_2 conc. (% ID·g^{-1} tiss.)	0.026 ± 0.006	0.032 ± 0.011	0.036 ± 0.007	0.019 ± 0.002	0.038 ± 0.006
skeleton	TiO_2 conc. (ng·g^{-1} tiss.)	4.18 ± 0.53	3.02 ± 0.57	6.02 ± 1.05	18.43 ± 2.50	17.71 ± 2.90
soft tissue	raw data (% ID)	0.44 ± 0.07	0.51 ± 0.05	0.352 ± 0.07	0.71 ± 0.13	0.68 ± 0.14
soft tissue	w/o resid. blood cont.	0.34 ± 0.05	0.43 ± 0.05	0.30 ± 0.07	0.70 ± 0.13	0.67 ± 0.14
soft tissue	w/o free 48V	0.32 ± 0.05	0.33 ± 0.07	0.15 ± 0.01	0.61 ± 0.13	0.67 ± 0.14
soft tissue	TiO_2 conc. (% ID·g^{-1} tiss.)	0.0014 ± 0.0002	0.0013 ± 0.0003	0.0007 ± 0.0001	0.0027 ± 0.0005	0.0029 ± 0.0006
soft tissue	TiO_2 conc. (ng·g^{-1} tiss.)	0.24 ± 0.02	0.16 ± 0.05	0.11 ± 0.01	2.54 ± 0.46	1.38 ± 0.32